Advances in Phase Retrieval by Transport of Intensity Equation

Dingfu Chen[1,2][a], Anand Asundi[2,3][b], Liansheng Sui[2,4][c], Chongtian Huang[2,3][d], Chi Wang[1] and Yingjie Yu[1]

[1]*Lab of Applied Optics and Metrology, Department of Precision Mechanical Engineering, Shanghai University, Shanghai, China*
[2]*Centre for Optical and Laser Engineering, School of Mechanical and Aerospace Engineering, Nanyang Technological University, Singapore, Singapore*
[3]*School of Computer Science and Engineering, Xi'an University of Technology, Xi'an, China*
[4]*d'Optron Pte Ltd, Singapore, Singapore*

Keywords: Transport of Intensity Equation, Transmission, Defocus Distance, Focus Plane, Magnification, High Order of Intensity Derivatives.

Abstract: There are many factors in the calculations of Transport of Intensity Equation, which may lead to the uncertainty of the retrieved phase. In this paper, effect of these parameters such as defocus distance, focus plane and magnification, on the results is studied. It is hoped that this would provide a more robust and reliable method for phase and optical height measurement. Furthermore, the effect of intensity derivatives calculated using two defocussed images as opposed to multiple images is also considered. A microlens array is chosen as the test sample in a commercial transmissive Transport of Intensity Equation system. From this study, it is concluded that the biggest factor influencing the result is the magnification, which is seen to provided totally different phase value for the same shape. Incorrect defocus distance or in-focus plane also lead to inaccurate reconstruction results while higher order differential provides better and more stable results than traditional two image differential.

1 INTRODUCTION

Quantitative phase imaging is finding diverse application both in the precision measurement and bio-medical imaging sectors. Non-interferometric quantitative phase retrieval such as coherent diffractive imaging (Williams et al., 2006) and Transport of Intensity Equations (Teague, 1983) provide greater flexibility in operation. Transport of Intensity Equation (TIE) is a two-dimensional second order elliptic differential equation proposed by Teague (Roddier, 1988), which provides a relationship between intensity and the phase of a light wave in the near Fresnel regime. In the past few decades, TIE has found a variety of applications in adaptive optics (Nugent et al., 1996), X-ray diffraction (Ishizuka and Allman, 2005), electron-microscopy (Streibl, 1984) and optical quantitative phase imaging (Zuo et al., 2013).

Basically, TIE needs at least three (under, in- and over focus) images or a series of through-focus intensity images (Nugent et al., 2011) (Soto and Acosta, 2007) (Waller and Tian, 2010) (Gureyev and Nugent, 1997). The in-focus intensity image contains no phase information; however, the variation of its intensity along the direction of propagation introduces phase contrast. In fact, any imaging system with a complex transfer function will provide some phase contrast. These images can then be inverted to quantitatively extract phase and amplitude.

For a paraxial beam propagating along the Z axis, the complex amplitude of the object is $\sqrt{I(x,y)}exp(ik\varphi(x,y))$, where $I(x,y)$ is the intensity and φ is the phase of the object wave. The derivative of intensity along the beam propagation

---

[a] https://orcid.org/0000-0002-8242-0644
[b] https://orcid.org/0000-0003-3835-4624
[c] https://orcid.org/0000-0002-1771-1664
[d] https://orcid.org/0000-0001-8081-7034

168

direction, Z, contains phase information that can be retrieved TIE. The general equation for TIE is (Blanchard and Greenaway, 1999):

$$-k\frac{\partial I(x,y)}{\partial z} = \nabla_\perp\big(I(x,y)\nabla_\perp\varphi(x,y)\big) \qquad (1)$$

where $I(x,y)$ is the intensity in the focal plane. k is the wave number. $\varphi(x,y)$ is the phase which needs to be calculated. $\nabla_\perp$ denotes the gradient operator over the propagation direction, z. Phase can be recovered from a measurement of intensity derivative along the optical axis and solving Eq. 1. The Fast Fourier Transform (FFT) method is widely used for solving the Poisson equations deduced from Eq. 1. If $I(x,y)$ is constant (i.e. a pure-phase object) and $\varphi(x,y)$ is continuous in a region with smooth boundaries, then the solution of the TIE is unique. The right side of the Eq. 1 can be rewritten as (Gorthi and Schonbrun, 2012) (Zuo et al., 2013) :

$$-k\frac{\partial I(x,y)}{\partial z} = \mathrm{I(x,y)}\nabla^2\varphi(x,y) \qquad (2)$$

the partial derivative in the left the side can be calculated in a finite difference manner as:

$$-k\frac{I(x,y,\Delta z) - I(x,y,-\Delta z)}{\Delta z} \qquad (3)$$

by recording two images spaced ±Δz on either side of focus (Soto and Acosta, 2007). For magnified images, the Δz at the object-plane is given as $\Delta z/M^2$.

Although a lot of researches have been done on TIE, the retrieval phase results still have some uncertainties based on the choice of Δz to obtain the derivative. A shorter Δz would approximate the derivative better but will be influenced by noise, while a larger Δz would smooth the result but would not be an accurate representative of the gradient. As in finite difference approaches, a series of images can be used to take advantage of the two cases. This paper would consider this and other effects such as magnification in the determination of phase.

2 EXPERIMENTAL SYSTEM

C. Zuo et al introduced an image relay system (Zuo et al., 2013) to replace the traditional mechanical translation of camera to record the out of focus images. This was commercialized by d'Optron Pte ltd (www.doptron.com) and has been applied for biological and industrial quantitative phase imaging. The system can be configured for both transmission and reflection measurement. It can be used as a stand-alone system or can be adapted onto any microscope

for increased spatial resolution. The axial resolution of the system is in the order of tens of nm. Figure 1 shows both the transmission and reflection stand-alone system, while Figure 2(a) shows the system as adapted to a microscope. The system has its own software shown in Figure 2(b) which allows the user to manipulate the defocus planes as well as record a series of images as desired. It also has the capability of getting depth from focus for samples with large depths.
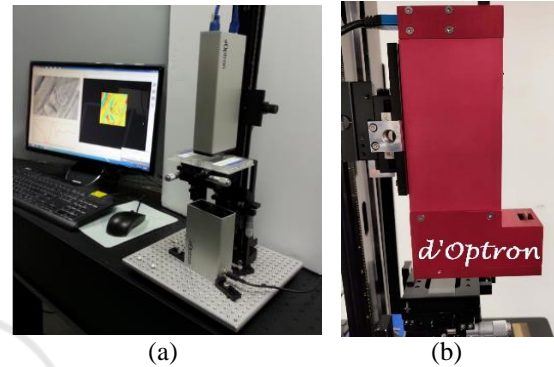

Figure 1: Stand-alone d'Nanoimager systems for (a) transparent samples and (b) reflecting samples.
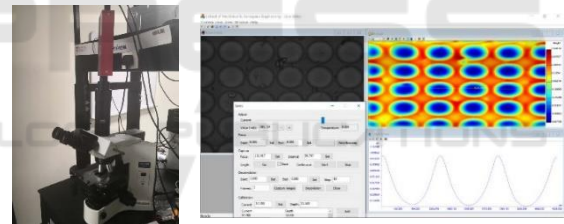

Figure 2: (a) d'Nanoimager adapted to a microscope. (b) Software interface.

3 EXPERIMENTAL SYSTEM

For this study, the d'Nanoimager is coupled to the conventional Olympus BX41 transmission microscope. A microlens array is measured using this system. The size of the microlens array is 10mm×10mm. The lens pitch is 75 μm. The software allows a large number of images and different focus distances to be rapidly recorded. Figure 3 shows a sample of over 100 through focus images. Three such image stacks were recorded using the same setup at different magnification of $10\times$, $20\times$, $40\times$, respectively which could be analysed in a variety of ways.
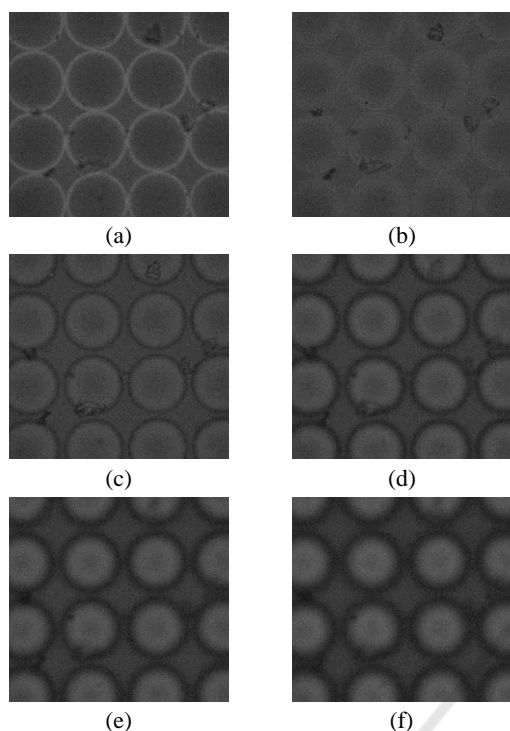
(a)   (b)

(c)   (d)

(e)   (f)

Figure 3: A series of through focus intensity images at 20× magnification of a microlens array.

3.1 Effect of Defocus Distance

As observed earlier, when Δz is large, the finite difference approximation breaks down while for smaller Δz leads to increased noise. Images at different defocus distances ranging from 0.8 μm to 23.0 μm were chosen from the stack with the 25th image (Figure 3(b)) being the in-focus image. As expected, when the defocus distance is small (Figure 4 (a)), the reconstruction was noisy which smoothed as the defocus distance increased (Figure 4(b)). However, the image tends to blur as the defocus distance increases.

3.2 Effect of Focus Plane

The influence of choice of in-focus image, I_0 , on the experiment results is considered next. To verify this, from the above image stack different in-focus image planes are selected. To avoid effects of Δz, the defocus distance was set to 7.7 μm, which was the optimal distance as per Section 3.1. Different in-focus planes ranging from the bottom to the top of microlens were selected from the same stack as earlier. As seen in Figure 5, changes in the in-focus image plane leads to a few changes in reconstructed phase. The phases in Figure 5(a-c) looks quite similar but their height values are different. While in Figure 5(d) where the in-focus
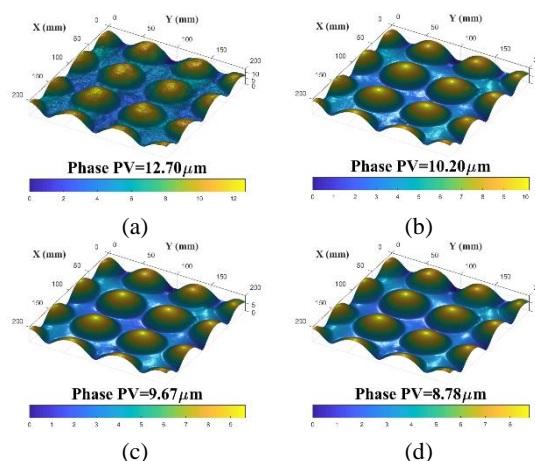

Phase PV=12.70μm   Phase PV=10.20μm

(a)   (b)

Phase PV=9.67μm   Phase PV=8.78μm

(c)   (d)

Figure 4: Phase retrieval using different defocus distance. (a) Δz=0.8 μm. (b) Δz=7.7 μm. (c) Δz=15.3 μm. (d) Δz =23.0 μm.

plane was on top of the microlens, the phase does not accurately describe the shape of an object.

To clearly highlight the effects of in-focus image and defocus distance, line plots of retrieved phase as function of the in-focus image plane are plotted as shown in Figure 6 for different defocus distance. As the number of images in the stack are fixed a larger defocus distance means fewer focus planes are available. So, the green line is the shortest and the blue line is the longest. It is interesting to note that the peak shifts to the right for increasing defocus distance and there is a reduction in the Peak to Valley (P-V) value, indicating smoothing of the result. Also, if the in-focus image is chosen at the wrong plane, the defocus images do not contain the entire information of the surface of the microlens array, resulting in lower phase values.
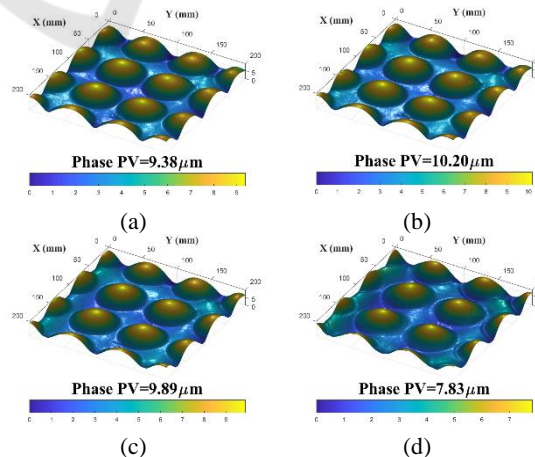

Phase PV=9.38μm   Phase PV=10.20μm

(a)   (b)

Phase PV=9.89μm   Phase PV=7.83μm

(c)   (d)

Figure 5: Phase retrieval with different in-focus image plane. (a) Focus at the background of microlens 20th (b) focus at the bottom of microlens 30th. (c) focus at the 50th plane. (d). focus at the 80th plane of microlens.
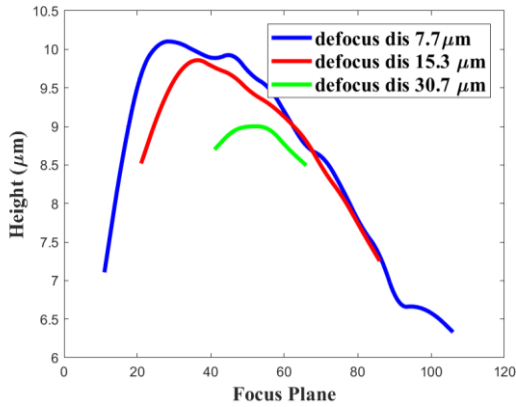
Figure 6: Effect of in-focus image and the defocus distance.

3.3 Effect of Magnification

For this hypothesis, experiments were conducted at 10×, 20×, 40× magnification. Figure 7 shows typical recorded intensity images. Due to the magnification, the Δz at the object plane for a 40× system is 6.2 μm, smaller than the height of the microlens.
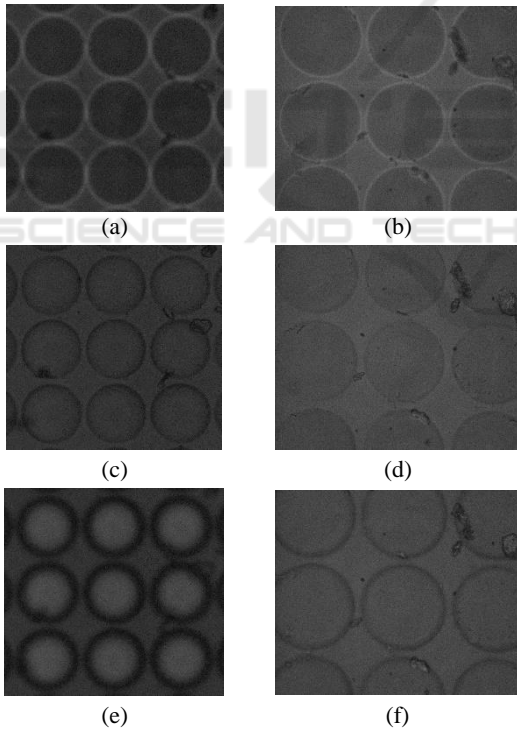

Figure 7: Intensity images of 10× magnification. (a) -26 μm under-focus image. (c) in-focus image. (e) +26 μm over-focus. Intensity images of 40× magnification with defocus distance (b) -3.10 μm (d) focus image. (f) +3.10 μm.
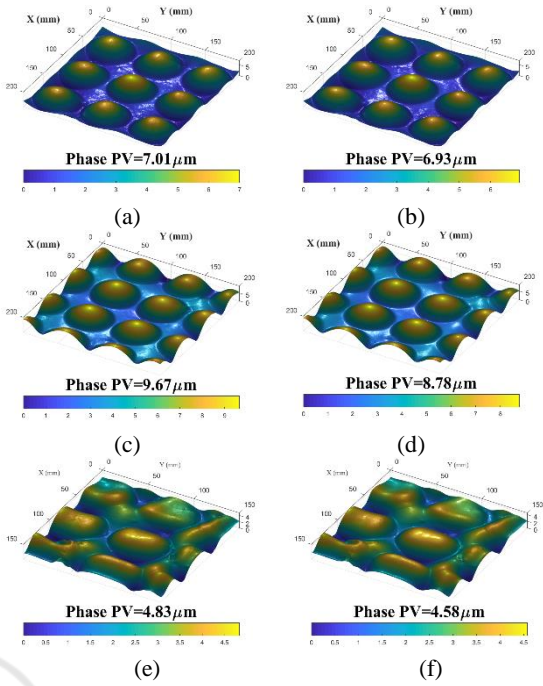

Figure 8: Phase retrieval of different magnification. (a) 10×, Δz =15.7 μm (b) 10×, Δz =26 μm (c) 20×, Δz =7.7 μm. (d) 20×, Δz =15.3 μm. (e) 40×, Δz =5.0 μm. (f) 40×, Δz =9.9 μm.

3.4 Effect of Multiple Defocus Images

Waller (Soto and Acosta, 2007) demonstrated a method for improving the accuracy of phase retrieval based on TIE by using multiple images to estimate the derivative:

$$\frac{\partial I}{\partial z} \approx \frac{a_{-n}I_{-n} + \cdots + a_0 I_0 + \cdots + a_n I_n}{\Delta z} \quad (4)$$

where a_n is the image weighting, I_n is the intensity image at $z = n\Delta z$, with I_0 as the focused image, negative n corresponds to under focus images, and positive n corresponds to over focus images. So, 2n+1 is the total number of the images and is the order of the derivatives.

In this step, we chose two groups of data - at 10× and 20× magnification. For the 20× dataset, 3, 7 and 15 images with defocus distances of 7.7 μm, 0.77 μm and 0.77 μm respectively and the in-focus image being the 30th image in the stack were selected. Figure 9(a-c) shows that the results are very close. For the 10× dataset, 7 and 15 images with a 2.67 μm defocus distance was tested with the in-focus image being the 30th image in the stack. Figure 9(d, e) shows consistent results. In order to clearly see the difference between the phase retrieved by 7 and 15

images, the difference of Figure 9(d) and Figure 9(e) show a PV deviation of 0.085μm.

Higher order TIE results show better quality than the lower order ones. However, too many images also blur the phase. The traditional TIE with 3 images is hidden behind low frequency noise and artifacts, while the retrieval phase with 15 images leads to the nonlinear error. Using 7 images seems to be a good compromise.
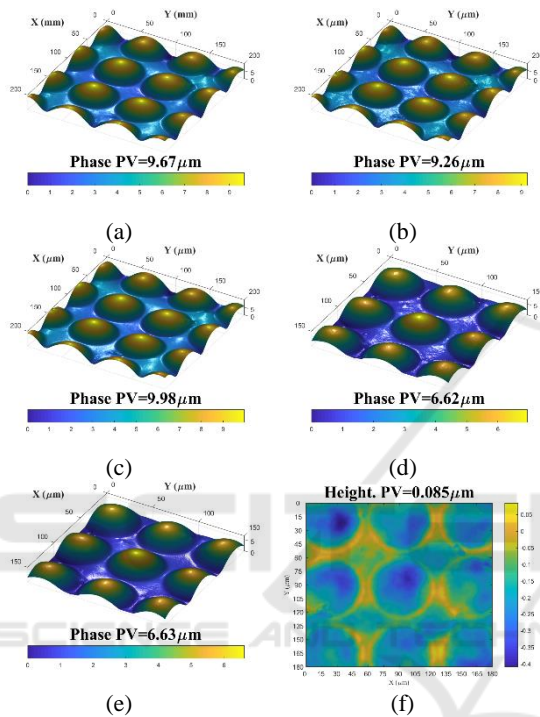

Figure 9: Phase retrieval using (a) 3 images, 20×, Δz =7.7 μm focus at the 30th plane. (b) 7 images, 20×, Δz =0.383 μm focus at the 30th plane. (c) 15 images, 20×, Δz =0.767 μm focus at the 30th plane. (d) 7 images, 10×, Δz =2.67 μm focus at the 30th plane. (e) 15 images, 10×, Δz =2.67 μm focus at the 30th planes. (f) the deviation between (d) and (e).

3.5 Effect of Reflective TIE

Transmissive TIE will be affected by the phase of the bottom surface which may also affect the final phase calculation. The d'Nanoimager is coupled to a Olympus reflective microscope at 10× magnification as shown in Figure 10(a), to measure top surface only. Figures 10(b-d) show typical recorded intensity images at different planes. As can be seen, due to the curvature of the lens, the top part appears to be too bright which would affect the calculation. The dust on the surface of the microlens array, helped identify the 50th image as the in-focus image.
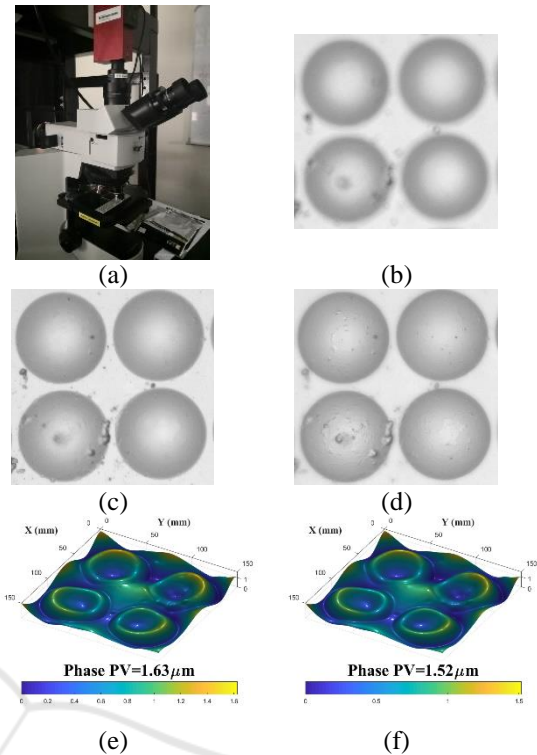

Figure 10: a serial of intensity images with reflective microscope. (a) d'Nanoimager adapted to a reflective microscope. (b) -15.7μm under-focus image. (c) in-focus image. (d) 15.7μm over-focus image. (e) the retrieved phase. (f) the retrieved phase with 23.6 μm defocus distance.

From the Figure 10(e, f), it is observed that the central part results are not correct – which could be due to the over-saturation of intensity resulting in little or no variation between the different images.
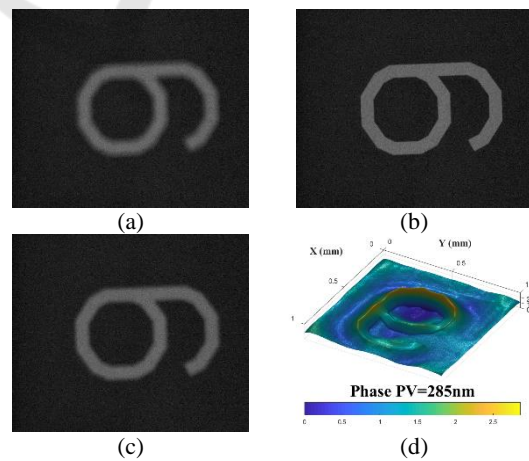

Figure 11: Intensity images with reflective microscope. (a) -163 μm under-focus image. (b) the in-focus image. (c) 163 μm over-focus image. (d) the retrieved phase using 31 images.

To confirm this a USAF target is also chosen as a sample to be measured with 5× magnification (Figure 11). Since the image was noisy, 31 terms were used to calculate the intensity derivative. Δz between the adjacent image is 10.8 μm . The result shows the good performance of the TIE, except for the sharp boundary points.

4 CONCLUSIONS

In this paper, the effect of different parameters on the retrieved phase by TIE method is explored. Using the commercial system from d'Optron, image stacks can be quickly collected. The greatest impact was from the magnification effect, which caused the largest change in the measured height. Other aspects of the magnification need to be further studied. Besides, the effect of the defocus distance and the choice of the in-focus plane also affects the result. We must ensure that the three images must span the entire height of the surface, otherwise, the retrieved phase is incorrect. Furthermore, using more terms to calculate the derivative can get more stable result. However, excessive number of images will offset the impact of noise and smooth the phase. About 7 images appears to be an optimal number. The reflective setup would be affected by large intensity variations especially if the curvature of the surface is large, however for flatter object such as the USAF target the results are quite good.

REFERENCES

Williams, G. J., Quiney, H. M., Dhal, B. B., Tran, C. Q., Nugent, K. A., Peele, A. G., Paterson, D., Jonge, M. D., 2006. Fresnel Coherent Diffractive Imaging. *Phys. Rev. Lett.* 97(2), 025506.

Teague, M. R., 1983. Deterministic phase retrieval: a Green's function solution. *J. Opt. Soc. Am.* 73(11), 1434–1441.

Roddier, F., 1988. Curvature sensing and compensation: a new concept in adaptive optics. *Appl. Opt.* 27(7), 1223–1225

Nugent, K. A., Gureyev, T. E., Cookson, D. J., Paganin, D., Barnea, Z., 1996. Quantitative phase imaging using hard X rays. *Phys. Rev. Lett.* 77(14), 2961–2964

Ishizuka, K., Allman, B., 2005 Phase measurement of atomic resolution image using transport of intensity equation. *J. Electron Micros.* 54(3), 191–197.

Streibl, N., 1984. Phase imaging by the transport equation of intensity, *Opt. Comm.* 49(1), 6–10.

Zuo, C., Chen, Q., Qu, W. J., Asundi, A., 2013. Noninterferometric single-shot quantitative phase microscopy. *Opt. Letter.* 38(18), 3538–3541.

Nugent, K., Paganin, D., Gureyev, T., 2001. A phase odyssey. *Physics Today* 54, 27–32.

Soto, M., Acosta, E., 2007. Improved phase imaging from intensity measurements in multiple planes. *Appl. Opt.* 46, 7978–7981.

Waller, L., Tian, L., Barbastathis, G., 2010. Transport of intensity phase-amplitude imaging with higher order intensity derivatives. *Opt. Express.* 18, 12552–12561

Gureyev, T., Nugent, K., 1997. Rapid quantitative phase imaging using the transport of intensity equation. *Opt. Comm.* 133(1-6), 339–346.

Blanchard, P. M., Greenaway, A. H., 1999. Simultaneous multiplane imaging with a distorted diffraction grating. *Appl. Opt.* 38, 6692–6699.

Gorthi, S. S., Schonbrun, E., 2012. Phase imaging flow cytometry using a focus-stack collecting microscope. *Opt. Lett.* 37, 707–709.

Zuo, C., Chen, Q., Qu, W., Asundi, A., 2013. High-speed transport of -intensity phase microscopy with an electrically tunable lens. *Opt. Express.* 21(20), 24060-24075.

d'Nanoimager by d'Optron Pte Ltd., www.doptron.com.